

T-shaped Ni⁰ Systems Featuring Cationic Tetrylenes: Direct Observation of L/Z-type Ligand Duality, and Alkene Hydrogenation Catalysis

Annika Schulz, Till L. Kalkuhl, Philip M. Keil, and Terrance J. Hadlington*

Abstract: We report a facile synthetic method for accessing rare T-shaped Ni⁰ species, stabilised by low-coordinate cationic germylene and stannylene ligands which behave as Z-type ligands toward Ni⁰. An in-depth computational analysis indicates significant Ni^d→E^p donation (E=Ge, Sn), with essentially no E→Ni donation. The tetrylene ligand's Lewis acidity can be modulated in situ through the addition of a donor ligand, which selectively binds at the Lewis acidic tetrylene site. This switches this binding centre from a Z-type to a classical L-type ligand, with a concomitant geometry switch at Ni⁰ from T-shaped to trigonal planar. Exploring the effects of this geometry switch in catalysis, isolated T-shaped complexes **3a–c** and **4a–c** are capable of the hydrogenation of alkenes under mild conditions, whilst the closely related trigonal planar and tetrahedral Ni⁰ complexes **5**, **D**, and **E**, which feature L-type chloro- or cationic-tetrylene ligands, are inactive under these conditions. Further, addition of small amounts of N-bases to the catalytic systems involving T-shaped complexes significantly reduces turnover rates, giving evidence for the in situ modulation of ligand electronics for catalytic switching.

Introduction

The coordination chemistry of the heavier tetrylenes has formed an important corner-stone in modern organometallic chemistry. Even before the seminal discovery of N-heterocyclic carbenes (NHCs) as stable divalent carbon species,^[1] Lappert had shown that related heavier congeners can be readily accessed through non-trivial protocols.^[2,3] Since that time, a diverse array of coordination complexes of these stable L-type Si^{II},^[4] Ge^{II},^[5] Sn^{II},^[6] and even Pb^{II}^[7] ligands

with transition metal (TM) fragments have been developed. Classically, TM fragments behave as Lewis acids (i.e. Z-type ligands), so forming dative interactions with tetrylene-centred lone electron pairs. For low-coordinate tetrylenes (i.e. non-base stabilised), back-bonding from the transition metal to the tetrylene centre forms a degree of E-TM π -bonding (E=Si, Ge, Sn), as per Fischer-type carbenes. This is perturbed on addition of a base to the E centre,^[8,9] or further *strengthened* on forming cationic tetrylene-TM complexes, whereby a linear alkylidyne-type structure is favoured, pertaining to E-TM triple bond interactions.^[10] Although rare, TM centres can also behave as Lewis *basic*, L-type ligands,^[11] culminating, for example, in metal-only Lewis pairs,^[12] and even TM-only “frustrated” Lewis pairs.^[13] Until recently, L-type bonding was unknown for Ni⁰, despite its electron-rich d¹⁰ ground state, and the well-established Lewis basicity of d¹⁰ Pd and Pt compounds.^[14] Classical base-free tetrylene complexes of Ni have been known for some time, typically featuring trigonal planar geometries at the E^{II} centres, and tetrahedral or trigonal planar geometries at Ni⁰, for 3-coordinate and 4-coordinate systems, respectively.^[5,15,16] However, it has additionally been shown that heavier tetrylenes have the capacity to switch the coordination nature of the bound Ni⁰, from a classical Lewis acceptor to a Lewis donor (i.e. TM→E; Figure 1a). In 3-coordinate Ni⁰ species, this has led to the discovery of geometrically distinct T-shaped Ni⁰ complexes, in which the Ni centre in fact behaves as a Lewis basic *donor* to the vacant *p*-orbital of the E^{II} centre, i.e. the E^{II} centre behaves as a Z-type ligand.^[17–19] Ni⁰ complexes bearing this structural motif remain extremely rare, the only reported examples being the bis-NHC-supported Cl₂Ge-Ni complex **A** reported by Roesler et al.,^[17] and both neutral and cationic silylene complexes **B** and **C** reported by Kato et al. (Figure 1b).^[18,19]

The propensity for a nickel(0)-tetrylene complex to adopt a T-shaped geometry increases with the heightened Lewis acidity and reduced nucleophilicity of the tetrylene centre. Indeed, heavier EX₂ fragments (E=Ge, Sn; X=Cl, Br) are known to behave as electrophiles in the coordination sphere of TMs,^[20] whilst even N-heterocyclic plumblylenes can behave as Lewis acidic Z-type ligands,^[21] in stark contrast to strongly nucleophilic, σ -donating NHCs. Still, despite their high Lewis acidity, utilising cationic tetrylenes does not typically favour Z-type ligand behaviour, but rather leads to the formation of alkylidyne complexes, featuring E-TM triple bonds.^[10] In fact, TM complexes featuring formally cationic tetrylene ligands are very rare indeed, and

[*] A. Schulz, T. L. Kalkuhl, P. M. Keil, Dr. T. J. Hadlington
 Fakultät für Chemie, Technische Universität München
 Lichtenberg Strasse 4, 85747 Garching (Germany)
 E-mail: terrance.hadlington@tum.de

© 2023 The Authors. Angewandte Chemie International Edition published by Wiley-VCH GmbH. This is an open access article under the terms of the Creative Commons Attribution Non-Commercial License, which permits use, distribution and reproduction in any medium, provided the original work is properly cited and is not used for commercial purposes.

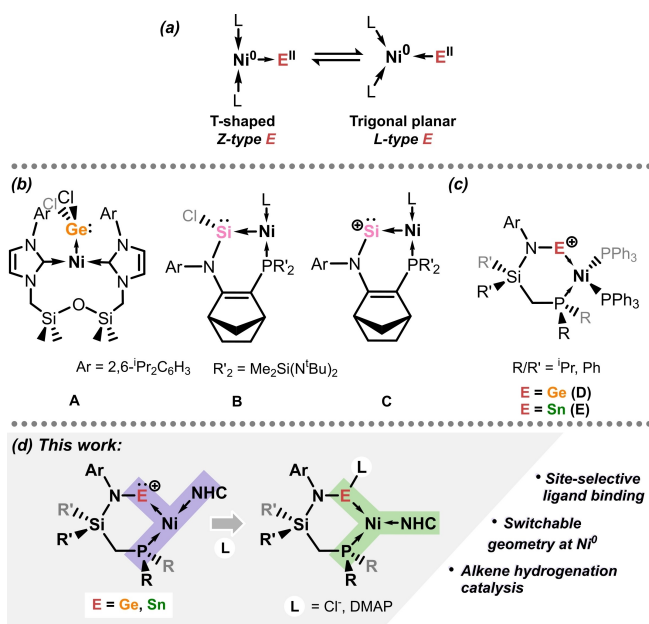


Figure 1. a) L/Z-type ligand duality in tetrylene- Ni^0 complexes, and its effect on geometry at Ni; b) Known examples of T-shaped Ni^0 complexes (A–C); c) Our previously reported cationic tetrylene Ni^0 complexes (D, E); d) This work.

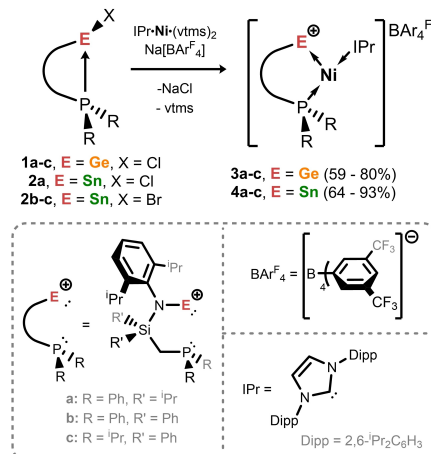
are largely exemplified by our own earlier work (*viz.* **D** and **E**, Figure 1).^[22,23] The cationic tetrylene centres in those systems behave as strong σ -donor ligands, whilst remaining highly Lewis acidic. They can therefore selectively bind incoming nucleophiles at the ligand's binding centre, so quenching their Lewis acidity. Given the small calculated barrier between T-shaped and trigonal planar geometries in silylene-nickel(0) complexes,^[19] we hypothesised that this ligand-centred nucleophile binding may act as a switch for Ni-centred conformational exchange.

Here, we report our efforts toward this end, in the development of a family of three-coordinate T-shaped Ni^0 complexes bearing low-coordinate, cationic tetrylene ligands. In these complexes, the Ni-centre acts as a Lewis basic donor towards the cationic E^{II} centres ($\text{E} = \text{Ge}, \text{Sn}$). These complexes react with classical π -acceptor ligands (e.g. RNC ; CO) through binding at Ni, whilst *N*-donor ligands bind selectively at the E^{II} centres. This latter site-selective binding leads to a geometry switch at Ni, from T-shaped to trigonal planar, in line with the reduced Lewis acidity of the tetrylene centres upon base-coordination. Steps towards employing such switchability in a catalytic regime are also outlined, in alkene hydrogenation catalysis which can be halted through addition of small amounts of *N*-donor ligands, and “restarted” through donor removal.

Results and Discussion

Accessing T-Shaped Ni^0 Complexes

In order to investigate the potential non-innocent behaviour of low-coordinate tetrylene ligands, we have developed a range of chelating phosphine-functionalised tetrylene systems, which we have previously shown to form 4-coordinate Ni^0 complexes (e.g. **D** and **E**, Figure 1).^[22,24] Extending this to lower coordinate Ni^0 complexes, we have utilised the readily accessible NHC- Ni^0 species, $\text{IPr}\cdot\text{Ni}[\eta^2\text{-(vtms)}]_2$ ($\text{IPr} = [(\text{Dipp})\text{NC}(\text{H})]_2\text{C}$; $\text{vtms} = \text{C}_2\text{H}_3\text{SiMe}_3$),^[25] which behaves as an efficient $[\text{IPr}\cdot\text{Ni}]$ transfer reagent.^[26] One-pot reaction of this Ni^0 precursor with equimolar amounts of halo-tetrylenes $\text{RR}'\text{DippEX}$ ($\text{E} = \text{Ge}, \text{X} = \text{Cl}$ (**1a–c**); $\text{E} = \text{Sn}, \text{X} = \text{Cl}$ (**2a**), $\text{X} = \text{Br}$ (**2b–c**)); $\text{RR}'\text{Dipp} = \{[\text{R}_2\text{PCH}_2\text{Si}(\text{R}')_2](\text{Dipp})\text{N}\}$; $\text{R}/\text{R}' = \text{Ph}, ^i\text{Pr}$; $\text{Dipp} = 2,6\text{-}^i\text{Pr}_2\text{C}_6\text{H}_3$) and $\text{Na}[\text{BAR}_4^{\text{F}}]$ ($\text{Ar}^{\text{F}} = 3,5\text{-}(\text{CF}_3)_2\text{C}_6\text{H}_3$) leads to elimination of vtms, and formation of deep purple reaction mixtures, which we believed to be indicative of the formation of cationic tetrylene- Ni^0 complexes **3a–c** (Ge) and **4a–c** (Sn; Scheme 1). $^{31}\text{P}\{^1\text{H}\}$ NMR spectra of crude reaction mixtures indicated the formation of a single new species in all cases (e.g. for **1a**: $\delta = 7.0$ ppm; for **3a**: $\delta = 10.4$ ppm).^[27] Following filtration of reaction mixtures, solvent removal, and addition of pentane to resulting purple oils, deep red-purple crystalline solids could be obtained. UV/Vis analysis of **3a** and **4a** revealed strong absorptions at 363 nm ($\epsilon = 17940 \text{ L mol}^{-1} \text{ cm}^{-1}$) and 365 nm ($\epsilon = 7420 \text{ L mol}^{-1} \text{ cm}^{-1}$), respectively. Upon structural characterisation of these products, it was found that, remarkably, all examples bear a T-shaped geometry at Ni^0 (Figure 2),^[28] rather than the trigonal planar geometry typically observed for 3-coordinate Ni^0 species.^[16] Such a geometry for Ni^0 is only known for three reported species, i.e. **A–C**,^[17–19] whilst no examples have been observed previously featuring Sn^{II} ligands. This geometry is observed due to the cationic tetrylene centres behaving as Z-type ligands, driving $\text{Ni}^0 \rightarrow \text{E}^{\text{II}}$ donation, as opposed to the typical $\text{E}^{\text{II}} \rightarrow \text{Ni}^0$ donation observed in tetrylene complexes of transition metals. The T-



Scheme 1. One-pot synthetic access to T-shaped Ni^0 complexes **3a–c** (Ge) and **4a–c** (Sn).

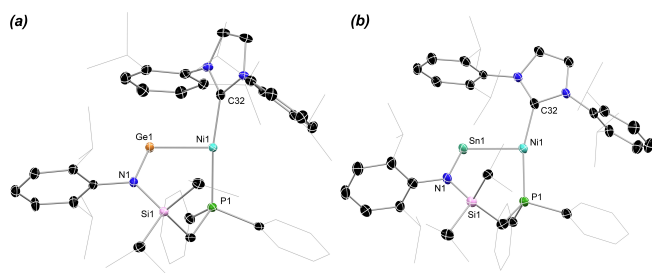


Figure 2. Molecular structures of the cationic part in a) **3a** and b) **4a**, with hydrogen atoms omitted, and thermal ellipsoids at 25% probability. Selected bond length [Å] and angles [°] for **3a**: Ge1–Ni1 2.269(1); P1–Ni1 2.185(1); C32–Ni1 1.923(4); Ge1–N1 1.846(4); C32–Ni1–P1 170.3(1); N1–Ge1–Ni1 109.7(1); Ge1–Ni1–P1 89.94(5); Ge1–Ni1–C32 98.2(1). For **4a**: Sn1–Ni1 2.473(1); P1–Ni1 2.182(2); C32–Ni1 1.940(5); N1–Sn1 2.082(4); C32–Ni1–P1 163.6(2); N1–Sn1–Ni1 107.4(1); P1–Ni1–Sn1 91.08(5); C32–Ni1–Sn1 103.7(1).

shaped structural motif in these species is exemplified by the near linear $C^{NHC}\text{--Ni--P}$ angles at their cores (e.g. **3a**: 170.3(1)°; **4a**: 163.6(2)°). As in our previously reported systems featuring the $[RR'DippE]^+$ ligands,^[22a] the E and P centres chelate the Ni^0 centre. However, due to the reversed electronic nature of the $E^{II}\text{--}Ni^0$ bonding interaction, the E–Ni bonds in these T-shaped Ni^0 systems are elongated relative to their higher coordinate counterparts **D** and **E** (e.g. d_{NiGe} : **D** = 2.1908(9) Å, **3a** = 2.269(1) Å; d_{NiSn} : **E** = 2.4024(9) Å, **4a** = 2.473(1) Å). The N–E–Ni bending angles in **3** and **4** are also significantly more acute (e.g. \angle_{NGeNi} : **D** = 133.0(1)°, **3a** = 109.7(1)°; \angle_{NSnNi} : **E** = 124.3(1)°, **4a** = 107.4(1)°), indicative of reduced sp -mixing in these E–Ni interactions, and prominent lone-pair character at the E^{II} centres. As a whole, these observations indicate an even lower E–Ni bond

order in complexes **3** and **4** compared to our earlier reported examples, in which the geometrically enforced N–E–Ni bending angle already significantly reduces metal to ligand back bonding, so amplifying the Lewis acidity at E. In the present case, the apparent Lewis acidity at E is great enough to favour Z-type ligand character.

To gain further insights into the electronic nature of complexes **3** and **4**, Density Functional Theory (DFT) and Natural Bond Order (NBO) analyses were carried out on model complexes $[^{PhMe}XylE\text{--}Ni\text{--}IPr]^+$ (E = Ge, **3'**; E = Sn, **4'**; $^{PhMe}Xyl = \{[Ph_2PCH_2SiMe_2](Dipp)N\}^-$). Metrical parameters for optimised structures in **3'** and **4'** are in good agreement with those for structurally characterised examples. For both species, the HOMO (**3'**: –9.78 eV; **4'**: –9.76 eV) and LUMO (**3'**: –2.86 eV; **4'**: –2.98 eV) represent a lone electron pair at E, and the σ^* -orbital of the E–Ni bonding interaction, respectively (Figures S134 and S135 in ESI). The former orbital further reiterates the Ni→E bonding situation in these species. Notably, the described LUMO shows considerable localisation at both E and Ni, which would indicate that *both* are viable binding sites for additional Lewis basic ligands (see below). In addition, the LUMO+1 (**3'**: –2.56 eV; **4'**: –2.85 eV) represents a further vacant p -orbital at E. Calculated bond orders for **3'** and **4'** (MBO: **3'** = 1.00; **4'** = 0.79) are again in keeping with relatively weak E–Ni bonding, and are not indicative of multiple bond character. An NBO-derived second order perturbation theory analysis does not dissect the Ge–Ni interaction in **3'** as a donor-acceptor bond. In **4'**, however, the Sn–Ni interaction is treated as a dative interaction; a lone electron pair and two vacant p -orbitals are observed at Sn (Figure 3a–c), whilst a high d -character lone electron pair and the P–Ni σ -bond are key donor orbitals (Figure 3d–f). The donation of the described Ni-centred d -character lone-pair to a vacant p -

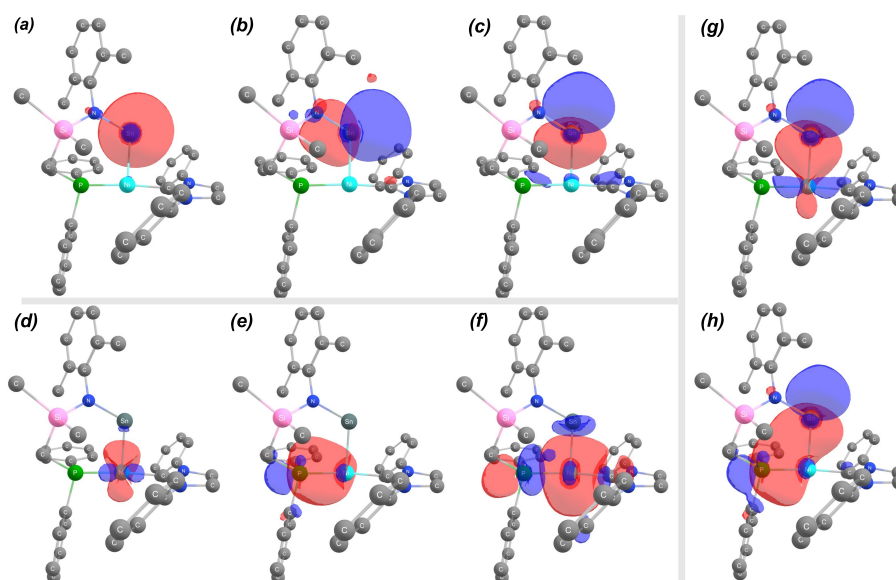


Figure 3. Orbitals involved in the Ni–Sn bonding interaction in **4'**, derived from an NBO second order perturbation theory analysis. (a) Sn-centred lone pair of electrons; (b), (c) Sn-centred vacant orbitals; (d)–(f) Ni-centred electron density; (g) = (d) + (c) [interaction energy of 88.40 kcal mol^{–1}]; (h) = (e) + (g) [interaction energy of 46.22 kcal mol^{–1}].

orbital on Sn (Figure 3g) shows a high interaction energy of $88.40 \text{ kcal mol}^{-1}$. Additional donation is found from the described P–Ni σ -bonding orbital, with a further $46.22 \text{ kcal mol}^{-1}$ binding energy (Figure 3h). Importantly, no significant Sn→Ni interactions are found. As such, these findings give key insights into the nature of the E–Ni bonds in these unique cationic Ge^{II} and Sn^{II} complexes featuring L-type Ni⁰ donor centres.

Ligand-Induced Geometry Switching

Following the isolation of T-shaped complexes **3** and **4**, we sought to further define the importance of the Lewis acidity at E in accessing this unusual geometry in Ni⁰ complexes. Our initial attempts to achieve this were in the synthesis of chloro-tetrylene complexes **5** (Ge) and **6** (Sn), through the addition of chloro-tetrylenes ^{Ph}₃P^{Ph}DippECl (E = Ge, Sn) to IPr·Ni[η²-(vtms)]₂ (Figure 4). Under these conditions, no reaction was observed. However, generating IPr·Ni(cod) (cod = 1,5-cyclooctadiene) at low temperatures,^[29] followed by addition of the desired chloro-tetrylene did lead to the formation of dark green reaction mixtures. On warming to ambient temperature, the germanium system retained its deep green colour, the formation of one major product indicated by ³¹P{¹H} NMR spectra of crude reaction mixtures. Reactions involving the chloro-stannylene, on the other hand, formed intractable mixtures at ambient temperature, and as such chloro-stannylene complex **6** could not be isolated. The related Ge system, **5**, was readily isolated as a dark green crystalline solid (Figure 4). Structural analysis of **5** rather interestingly indicates a *trigonal planar* Ni⁰ centre, in which the Ge^{II} centre has now switched from a Z-type to an L-type ligand, which we attribute to a reduction in the Lewis acidity of this Ge^{II} binding centre relative to that in **3**. This leads to a contraction of the Ge–Ni interaction ($d_{\text{GeNi}} = 2.217(1) \text{ \AA}$) relative to **3** (e.g. **3a**: $d_{\text{GeNi}} = 2.269(1) \text{ \AA}$), and a lessened bending angle at Ge (\angle_{NGeNi} in **5**: $120.9(1)^\circ$; in **3a**:

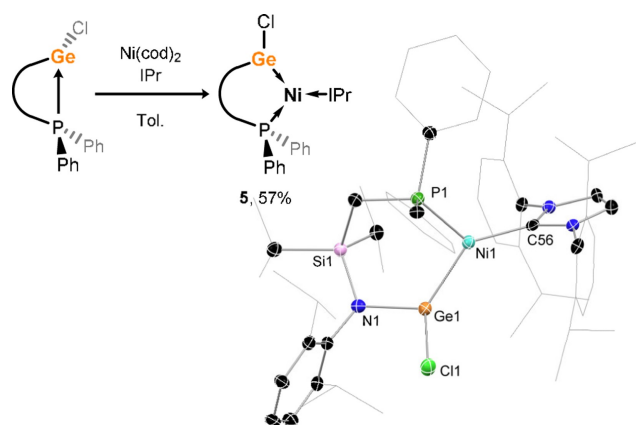
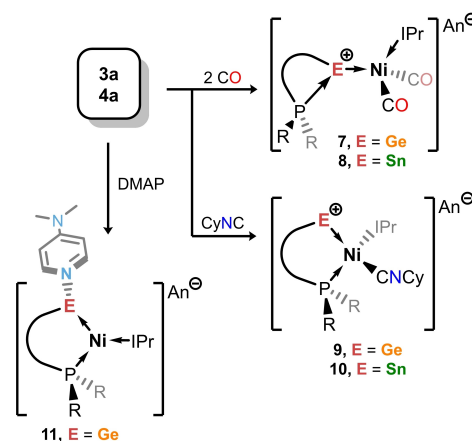


Figure 4. Synthetic access to trigonal planar Ni⁰-chlorotetrylene complex **5**, and the molecular structure of **5**. Selected bond length [Å] and angles [°] for **5**: Ge1–Ni1 2.217(1); C56–Ni1 1.940(6); P1–Ni1 2.138(2); N1–Ge1 1.891(5); C56–Ni1–P1 128.1(2); P1–Ni1–Ge1 94.89(5); C56–Ni1–Ge1 136.6(2); N1–Ge1–Ni1 120.9(1).

$109.7(1)^\circ$). Notably, this case is quite different to that observed in closely related silylene-Ni⁰ complexes recently reported by Kato et al. (*viz.* **B** and **C**, Figure 1), in which both the cationic and chloro silylene complexes are T-shaped at Ni. The ability for the geometry at Ni⁰ to switch in direct relation to the nature of the germylene in complexes described here thus has exciting potential for outer-sphere ligand effects in complex switchability.

To further probe this concept, we focused our efforts on forming adducts of cationic complexes **3** and **4** with differing donor ligands. This focused on the N-donor ligands NH₃ and N,N-dimethylaminopyridine (DMAP), and the π -acceptor ligands CO and CyNC (Scheme 2). This also raises the question: can site-selective ligand binding be observed, based upon the differing electronic nature of cationic E^{II} centres and Ni⁰ centres in these complexes? DFT-derived binding energies of differing N-donor ligands, CO, and MeNC to the E^{II} centre or Ni⁰ centre in model complexes **3'** and **4'** have been calculated, and are summarised in Table 1.^[30] For both **3'** and **4'** the binding of CO and MeNC at Ni⁰ is significantly favoured, by up to 69.9 kJ mol^{-1} , which is perhaps not surprising given that tetrylene adducts of CO are extremely rare.^[31] In contrast, the binding of ammonia in **3'** is in fact *favoured* at the Ge site by 10.5 kJ mol^{-1} , whilst



Scheme 2. Adduct formation in complexes **3a** and **4a** (An = BAR^F₄).

Table 1: Binding energies for ligands (L) to either Ni or Ge/Sn centres in model cationic-tetrylene Ni⁰ complexes.^[a]

L	3'		4'		D'	E'
	Ni binding	Ge binding	Ni binding	Sn binding		
CO	-47.0	13.7	-43.8	13.4	-	-
CNMe	-75.2	-5.3	-71.3	-18.4	-	-
NH ₃	-17.0	-27.5	-47.0	-42.0	-32.3 ^[b]	-37.9
NMe ₃	-7.6	-22.2	-	-	-	-
DMAP	-55.6	-72.8	-	-	-	-
Py	-27.7	-31.6	-	-	-	-

[a] Calculated at the ω B97XD//def2-SVP level of theory for all atoms. All energies given in kJ mol^{-1} . [b] Value taken from ref. [22a].

for **4'** binding at Sn or Ni has a similar energy. Ge-centred binding can be further favoured in employing the strong nitrogen base, DMAP, with a binding affinity at Ge of 72.8 kJ mol^{-1} , compared to 55.6 kJ mol^{-1} at Ni. Experimentally, the site-selective ligand binding capacities of **3** and **4** are satisfyingly in-keeping with computational results. The addition of CO to solutions of **3a** or **4a** leads to binding of CO at the Ni centres in these complexes. Using an excess of CO rather leads to complete elimination of the group 14 ligands, $[\text{P}^{\text{hiP}}\text{DippE}][\text{BAR}^{\text{F}}_4]$, as shown by $^{31}\text{P}\{^1\text{H}\}$ NMR spectroscopic analysis.^[24] Careful addition of ≈ 2 equiv instead allows for the isolation of bis-CO complexes **7** (Ge) and **8** (Sn), with the chelating phosphine arm in these species now binding the cationic tetrylene centres, as indicated by structural analysis (Figures 5a and S121). These species therefore bear 4-coordinate tetrahedral Ni^0 centres, and 3-coordinate E^{II} centres, with E–Ni distances in keeping with those expected for dative $\text{E} \rightarrow \text{Ni}$ single bonds. Moving to the sterically larger isocyanide, CyNC, facilitates mono-addition at Ni, in the formation of complexes **9** and **10**, in which the chelating phosphine arm remains bound to the Ni centre. Again, structural analysis of these species reveals tetrahedral Ni^0 centres, with low-coordinate cationic E^{II} centres similar to those found in our previously reported complexes **D** and **E** (Figures 5b and S121). A notable contraction in E–Ni bond lengths is now observed (**9**: $2.1890(9) \text{ \AA}$; **10**: $2.422(1) \text{ \AA}$), as well as an opening of the N–E–Ni angles (**9**: $128.29(8)^\circ$; **10**: $118.42(9)^\circ$), both indicative of a switch to L-type tetrylene bonding centres, and a degree of donor-acceptor bonding between E and Ni in these moieties, as described in our earlier reports.^[22a]

In contrast to the addition of π -acceptor ligands, and again in line with calculated binding values, *N*-donor ligands selectively bind at the cationic tetrylene centres. Addition of ammonia to solutions of **3a** or **4a** at low temperature leads to the formation of deep green solutions, similar in colour to chloro-germylene complex **5**. In situ $^{31}\text{P}\{^1\text{H}\}$ spectra for the addition of NH_3 to **3a** at -40°C ($\delta = 18.7 \text{ ppm}$) suggest the formation of a single species (Figure S88 in Supporting

Information). Whilst complex mixtures form upon warming to RT, this gave us early circumstantial evidence for binding at Ge/Sn. Moving to an aprotic *N*-base, addition of DMAP to solutions of **3a** leads only to binding at the Ge site, in the formation of **11**.^[32] This compound crystallises as deep blue-purple plates, structural analysis of which indicates a single DMAP ligand bound at the Ge^{II} centre in this compound. ^1H NMR spectra of dissolved **11** are highly broadened (Figure S82 in Supporting Information), presumably due to hindered rotation caused by the introduction of considerable steric hinderance at the Ge centre in this compound. Nevertheless, one clear signal can be observed in the $^{31}\text{P}\{^1\text{H}\}$ NMR spectrum for this compound ($\delta = 18.9 \text{ ppm}$, Figure S83 in Supporting Information), in keeping with that observed for the above described NH_3 adduct, albeit also somewhat broadened. Importantly, the Ni^{II} centre in **11** now bears a trigonal planar geometry (Figure 5c), in line with our hypothesis that reduced ligand Lewis acidity can trigger such a geometric switch. As with chloro-germylene complex **5**, a contraction of the Ge–Ni distance ($2.208(2) \text{ \AA}$), and an opening of the N–Ge–Ni angle ($120.5(2)^\circ$) are both indicative of $\text{Ge} \rightarrow \text{Ni}$ donation, in line with a now L-type germylene ligand. These ligand binding studies in complexes **3** and **4** indicate that the Lewis acidic E^{II} binding site can indeed play a role in geometry modulation at Ni^0 , through site selective binding.

Alkene Hydrogenation Catalysis

Due to their unique, readily tuneable electronic nature, low-valent *p*-block species are extremely promising targets as a new generation of bespoke ligand systems,^[4c,8] particularly regarding metal-ligand cooperativity.^[23,33] Using these concepts for the development of novel catalytic systems based upon Earth-abundant elements forms a key aspect of our endeavours in the development of chelating tetrylene ligands, in which the tetrylene binding sites are strongly ambiphilic. As described, we have shown that small ligand

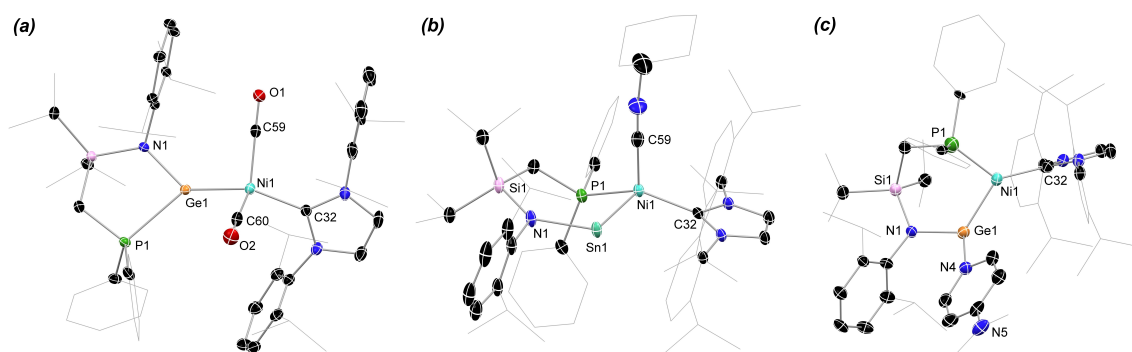


Figure 5. Molecular structure of a) **7**, b) **10**, and c) **11**, with hydrogen atoms omitted, and thermal ellipsoids at 24% probability. Selected bond lengths and angles for **7**: Ge1–Ni1 $2.260(1)$; C32–Ni1 $1.971(6)$; C59–Ni1 $1.824(6)$; C60–Ni1 $1.784(6)$; P1–Ge1 $2.542(2)$; N1–Ge1 $1.866(4)$; N1–Ge1–P1 $86.9(1)$; P1–Ge1–Ni1 $128.71(4)$; N1–Ge1–Ni1 $128.61(1)$; C32–Ni1–Ge1 $132.8(2)$; C59–Ni1–C60 $118.5(3)$. For **10**: Sn1–Ni1 $2.422(1)$; P1–Ni1 $2.185(1)$; C32–Ni1 $1.975(3)$; C59–Ni1 $1.839(5)$; N1–Sn1 $2.071(3)$; N1–Sn1–Ni1 $118.42(9)$; Sn1–Ni1–P1 $85.00(3)$; C32–Ni1–P1 $133.3(1)$; C32–Ni1–Sn1 $111.8(1)$. For **11**: Ge1–Ni1 $2.208(2)$; N1–Ge1 $1.866(8)$; N4–Ge1 $2.084(6)$; P1–Ni1 $2.12(2)$; C32–Ni1 $1.951(9)$; N1–Ge1–Ni1 $120.5(2)$; N1–Ge1–N4 $102.1(3)$; Ni1–Ge1–N4 $119.1(2)$; Ge1–Ni1–P1 $94.9(5)$; Ge1–Ni1–C32 $133.2(2)$; P1–Ni1–C32 $131.7(5)$.

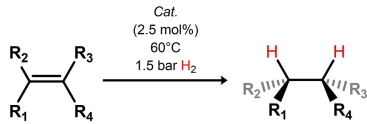
variations can lead to pronounced electronic differences at the TM centre. This, in turn, may affect the catalytic efficacy of a complex, highlighting the importance of ligand design in catalysis. Our previously reported complexes **D** and **E** showed the capacity to catalyse the hydrosilylation of unactivated alkenes. Here, we sought to extend this to more challenging catalytic alkene hydrogenation, using mild conditions (1.5 bar H₂, 60 °C, Table 2). Firstly, screening the addition of H₂ to vtms using either **D** or **E** as catalysts showed no catalytic turnover. Moving to the trigonal planar Ni⁰ complex **5**, in which the germylene behaves as an L-type ligand, again essentially no catalytic turnover was observed.^[34] Quite remarkably, in contrast, all T-shaped Ni⁰ complexes (i.e. **3a–c**, **4a–c**) were indeed found to be active in the described catalytic regime, in the clean formation of (ethyl)trimethylsilane with up to 99 % conversion (entries 1–8, Table 2). Reaction optimisation revealed complexes **3a** and **4a**, bearing the [P^{hi}P]Dipp ligand, to be the most active catalysts, with a modest 2.5 mol % loading. We note that for all systems, no reaction is observed when an excess of either H₂ or vtms is added to solutions of these complexes. Further, heating samples of pure **3a** and **4a** in the reaction solvent mixture (i.e. a 3:1 mixture PhF/C₆D₆) at 60 °C for 6 days showed no signs of catalyst decomposition (Figures S89–S92 in Supporting Information). Monitoring ¹H and ³¹P{¹H} NMR spectra of catalytic reactions also showed that **3a–c** and **4a–c** are the only observable species (Figures S97, S98 in Supporting Information), which would suggest that these are the resting state in the catalytic process.

Exploring substrate scope, both complexes were found to hydrogenate a range of terminal, internal, and branched alkenes. As observed with our earlier hydrosilylation studies, 1-hexene is both hydrogenated and isomerised to 2- and 3-hexene, with full consumption of 1-hexene observed within 1 h (entries 9 and 10, Table 2). Approximately 50 % of the hydrogenation product (i.e. hexane) is observed after this time. Bulky and highly substituted alkenes (e.g. diphenylethylene, tetramethylethylene, entries 19, 20, 27, and 28, Table 2) proved challenging for our systems, perhaps not surprising given the steric bulk of their ligand substituents. Nevertheless, more highly substituted alkenes (e.g. α - and β -methylstyrene) could be hydrogenated, as well as the bulky terminal alkenes, vtms and 3,3-dimethyl butene.^[35] We note that these catalysts do not compete with the state-of-the-art TM systems.^[36] As a proof-of-concept study, however, these results indicate that the cationic tetrylene ligands developed here (viz. [P^{RR}DippE]⁺), which in fact remain of great of fundamental interest in their own right, are capable of directing challenging hydrogenation catalyses in conjunction with nickel. Given the importance of developing new catalysts for transformations which rely on precious TMs,^[37] this forms a promising foundation for further developing novel main-group systems for affecting catalysis with Earth-abundant metals.

We then sought to investigate the effect of external *N*-donors on catalytic efficiency (Table 3, Figure S125 in Supporting Information). Given the observation, both computationally and experimentally, that such species bind the germylene centre in **3a**, switching from *Z*- to *L*-type

ligand character, we hypothesised that addition of an *N*-donor to the catalytic system should lead to a decrease in activity. Indeed, conducting catalysis in donor solvents (i.e. THF-d₈) greatly hampers catalysis, potentially for similar reasons (viz Figure S94 in Supporting Information). As *N*-donor ligands, we investigated triethyl amine (NEt₃) and 2,6-lutidine (Lut).^[38] As for NH₃ and DMAP, NMe₃ and pyridine, which are employed as models for NEt₃ and Lut, respectively, are computationally found to bind favourably at the Ge centre in model complex **3'** (Table 1). Addition of either NEt₃ or Lut to **3a** does not lead to obvious adduct formation, as ascertained by NMR spectroscopy,^[39] presumably due to the large steric profile of these donor species. We note, however, that the ¹H NMR signal for the Me-groups in Lut, when in the presence of **3a**, is highly broadened, likely indicating a rapid binding equilibrium (Figure S124 in Supporting Information). Catalytic hydrogenation of vtms with **3a** (2.5 mol %) was then conducted in the presence of NEt₃ (5 mol %) or Lut (5 and 50 mol %). Firstly, the donor-free system leads to a conversion of 77 % after 6 h. In the presence of 5 mol % NEt₃, a modest reduction in catalytic activity is observed after the same time, with conversion of 58 % (Figure S121 in Supporting Information). Lut, on the other hand, showed a much more pronounced effect: in the presence of 5 mol % Lut, just 17 % conversion is observed after 6 h (Figure S122 in Supporting Information), whilst addition of 50 mol % Lut leads to 11 % conversion after the same time (Figure S123 in Supporting Information). Whilst these results are indeed interesting, we note that this does not necessarily correlate with binding of the base at Ge, and could be due to alternative catalyst deactivation mechanisms.

In order to probe the true switchability of these systems, we wished to removed Lut from the catalytic systems and “restart” catalysis. Two methods were investigated here, coordination of Lut with Lewis acidic BPh₃ (Table 3, entry 5), and removal of Lut *in vacuo* (Table 3, entry 6). In both cases, catalysis was first carried out in the presence of 5 mol % Lut for 2 h, leading to \approx 5 % alkene conversion. The addition of BPh₃ to these solutions, followed by repressurising with H₂ and heating for 6 h, led only to a modest increase in conversion (viz. 29 %) when compared to the BPh₃-free system (viz. 17 %; Figure S126 in Supporting Information). In contrast, removal of Lut *in vacuo* had a much more pronounced effect (Figures S127, S128 in Supporting Information). Here, Lut was removed *in vacuo* at 60 °C for 30 min. The catalyst residue was then redissolved and its identity confirmed by ¹H and ³¹P{¹H} NMR spectroscopy. Alkene and H₂ were once again added to the sample, and the mixture heated for 6 h. After this time, 64 % alkene hydrogenation was observed, comparing well to the 77 % overserved in the blank donor-free reaction. It is worth noting here that described T-shaped Ni⁰ complexes are highly oxygen sensitive, and, given the small scale of these reactions, it can assumed that some catalyst decomposition occurs during removal of volatiles and redissolution. Overall, then, this set of results incites a switchable character in the catalytic hydrogenation achieved by these T-shaped Ni⁰ complexes. As mentioned above, whilst this does not

Table 2: Catalytic alkene hydrogenation utilising T-shaped Ni⁰ complexes.^[a]


entry	catalyst	substrate	t (h)	product	conversion (yield) ^[b]
1	3a		8		81
2	3b		8		24
3	3c		8		19
4	4a		8		47
5	4b		8		34
6	4c		8		39
7	3a		10		99
8	4a		11		99
9	3a		1		99 (50) ^[c]
10	4a		0.5		99 (46) ^[c]
11	3a		12		99 (38) ^[d]
12	4a		8		99 (42) ^[d]
13	3a		48		99 (83) ^[e]
14	4a		48		99 (76) ^[e]
15	3a		72		79
16	4a		72		42
17	3a		72		83
18	4a		72		53
19	3a		72		18
20	4a		72		25
21	3a		72		12
22	4a		72		13
23	3a		48		99
24	4a		48		97
25	3a		72		49 (12) ^[f]
26	4a		72		99 (30) ^[f]
27	3a		72		16
28	4a		72		15

[a] Conducted in gas-tight NMR tubes, as solutions in 0.4 mL (3:1 PhF/C₆D₆), 2.5 mol% cat., 60 °C, 1.5 bar H₂, and 0.02 mmol mesitylene as an internal standard. All reactions were run in triplicate; [b] Conversion denotes % consumption of substrate. Yield denotes % formation of given product, where other products were observed. Details of other products given in each case. All values are determined by integration of ¹H NMR spectra. [c] The remainder of 1-hexene is isomerised to 2- and 3-hexene. [d] The remainder of the octadiene is

Table 2: (Continued)

isomerised to internal alkenes. [e] We presume that the remaining styrene is polymerised. [f] The remainder of converted butadiene forms 2,3-dimethyl-1-butene (Ge: 26%, Sn: 29%) and 2,3-dimethyl-2-butene (Ge: 11%, Sn: 40%).

Table 3: The effect of N-donors on catalytic efficiency in alkene hydrogenation.^[a]

entry	additive (mol %)	substrate	t (h)	product	conversion
1	-		6		77
2	NEt ₃ (5)		6		58
3	Lut (5)		6		17
4	Lut (50)		6		11
5	Lut (5) + BPh ₃ (5) ^[b]		6		29
6	Lut (5), vacuum ^[c]		6		64

[a] Conducted in gas-tight NMR tubes, as solutions in 0.4 mL of a 3:1 mixture PhF/C₆D₆, with 0.02 mmol mesitylene as an internal standard, and the given donor added via micropipette. [b] Catalysis was run for 2 h in the presence of Lut, BPh₃ subsequently added, and catalysis continued for 6 h. [c] Catalysis was run for 2 h in the presence of Lut, and all volatiles removed in vacuo. The catalyst was then redissolved, and catalysis restarted (i.e. alkene and H₂ added), and monitored for 6 h.

directly correlate with a “geometry switch” in the presence of Lut, it is an interesting outcome which we believe to be related to the non-innocent character of single-centre ambiphile ligands, such as the cationic tetrylenes in **3** and **4**.

Conclusion

We disclose straight-forward methods for accessing a range of T-shaped Ni⁰ complexes, stabilised by low-coordinate cationic tetrylene ligands built into chelating binding scaffolds. The Ni⁰ centres in these species are shown to behave as donors towards the cationic E^{II} centres (E=Ge, Sn) through observation of solid-state metrical parameters, and supporting computational analyses. The small energy difference between T-shaped and trigonal planar Ni⁰ geometries allows for geometry switching through *in situ* modification of ligand electronics. That is, addition of a donor ligand at the cationic tetrylene centre switches the Ni⁰ geometry from T-shaped to trigonal planar. Further, all T-shaped complexes are shown to be effective in the catalytic hydrogenation of alkenes. Addition of N-donor ligands to the catalytic systems leads to a significant reduction in catalytic efficiency. Taken as a whole, these results provide evidence for switchable molecular catalysis through site-selective donor binding. We continue to investigate key mechanistic aspects of these systems, as well as broader catalytic applications.

Acknowledgements

T.J.H. thanks the Fonds der Chemischen Industrie (FCI) for generous funding of this research through a Liebig Stipendium, the DFG for an Independent Research grant (Project Nr. HA9030/3-1470323245), and the Technical University Munich for the generous endowment of TUM Junior Fellow Funds. T.L.K. thanks the Friedrich Ebert Foundation for receipt of a Master scholarship. We also thank M. Muhr and I. Antsiburov for the measurement of LIFDI-MS samples. Open Access funding enabled and organized by Projekt DEAL.

Conflict of Interest

The authors declare no conflict of interest.

Data Availability Statement

Data available in article supplementary material, and on reasonable request from the authors.

Keywords: Alkene Hydrogenation · Cationic Tetrylenes · Non-Innocent Ligands · Sustainable Catalysis · Switchable Molecules

- [1] E. O. Fischer, A. Maasbøll, *Angew. Chem. Int. Ed. Engl.* **1964**, *3*, 580–581.
- [2] M. F. Lappert, M. J. Slade, J. L. Atwood, M. J. Zaworotko, *J. Chem. Soc. Chem. Commun.* **1980**, 621–622.
- [3] T. Fjeldberg, H. Hope, M. F. Lappert, P. P. Power, A. J. Thorne, *J. Chem. Soc. Chem. Commun.* **1983**, 639–641.
- [4] For examples of base-free silylene transition metal complexes, see the following and references within: a) M. Denk, R. K. Hayashi, R. West, *J. Chem. Soc. Chem. Commun.* **1994**, 33–34; b) B. Gehrhus, P. B. Hitchcock, M. F. Lappert, H. Maciejewski, *Organometallics* **1998**, *17*, 5599–5601; c) Y.-P. Zhou, M. Driess, *Angew. Chem. Int. Ed.* **2019**, *58*, 3715–3728; d) “Compounds with Bonds Between Silicon and d-Block Metal Atoms”: T. J. Hadlington in *Comprehensive Organometallic Chemistry IV* (Eds.: G. Parkin, D. O’Hare, K. Meyer), Elsevier, Amsterdam, **2022**.
- [5] For examples of base-free germylene TM complexes, see: a) M. F. Lappert, S. J. Miles, P. P. Power, *J. Chem. Soc. Chem. Commun.* **1977**, 458–459; b) P. Jutzl, W. Steiner, E. König, *Chem. Ber.* **1978**, *111*, 606–614; c) F. Hupp, M. Ma, F. Kroll, J. O. C. Jimenez-Halla, R. D. Dewhurst, K. Radacki, A. Stasch, C. Jones, H. Braunschweig, *Chem. Eur. J.* **2014**, *20*, 16888–16898; d) K. E. Litz, J. E. Bender IV, J. W. Kampf, M. M. Banaszak Holl, *Angew. Chem. Int. Ed. Engl.* **1997**, *36*, 496–498; e) J. Li, C. Schenk, F. Winter, H. Scherer, N. Trapp, A. Higelin, S. Keller, R. Pöttgen, I. Krossing, C. Jones, *Angew. Chem. Int. Ed.* **2012**, *51*, 9557–9561.
- [6] For examples of base-free stannylene TM complexes, see: a) J. D. Cotton, P. J. Davison, D. E. Goldberg, M. F. Lappert, K. M. Thomas, *Chem. Commun.* **1974**, 893–895; b) P. B. Hitchcock, M. F. Lappert, M. C. Misra, *J. Chem. Soc. Chem. Commun.* **1985**, 863–864; c) T. A. K. Al-Allaf, C. Eaborn, P. B. Hitchcock, M. F. Lappert, A. Pidcock, *J. Chem. Soc. Chem. Commun.* **1985**, 548–550; d) J. J. Schneider, N. Czap, D. Bläser, R. Boese, *J. Organomet. Chem.* **1999**, *584*, 338–343; e) K. M. Krebs, S. Freitag, H. Schubert, B. Gerke, R. Pöttgen, L. Wesemann, *Chem. Eur. J.* **2015**, *21*, 4628–4638.
- [7] a) H. Arp, J. Baumgartner, C. Marschner, P. Zark, T. Müller, *J. Am. Chem. Soc.* **2012**, *134*, 10864–10875; b) P. W. Smith, R. C. Handford, T. D. Tilley, *Organometallics* **2019**, *38*, 4060–4065.
- [8] Silylenes and germylenes have can even be strong donor ligands than the ubiquitous N-heterocyclic carbenes. See: a) Z. Benedek, T. Szilvási, *RSC Adv.* **2015**, *5*, 5077–5086; b) Z. Benedek, T. Szilvási, *Organometallics* **2017**, *36*, 1591–1600.
- [9] This classic L-type ligand character is exemplified by the many TM complexes bearing the amidinato-silylene ligand scaffold. For examples, see: a) R. Azhakar, R. S. Ghadwal, H. W. Roesky, H. Wolf, D. Stalke, *J. Am. Chem. Soc.* **2012**, *134*, 2423–2428; b) A. Brück, D. Gallego, W. Wang, E. Irran, M. Driess, J. F. Hartwig, *Angew. Chem. Int. Ed.* **2012**, *51*, 11478–11482; c) D. Gallego, A. Brück, E. Irran, F. Meier, M. Kaupp, M. Driess, J. F. Hartwig, *J. Am. Chem. Soc.* **2013**, *135*, 15617–15626; d) S. Schäfer, R. Köppe, P. W. Roesky, *Chem. Eur. J.* **2016**, *22*, 7127–7133; e) R. Akhtar, S. H. Kaulage, M. P. Sangole, S. Tothadi, P. Parvathy, P. Parameswaran, K. Singh, S. Khan, *Inorg. Chem.* **2022**, *61*, 13330–13341.
- [10] A. C. Filippou, P. Ghana, U. Chakraborty, G. Schnakenburg, *J. Am. Chem. Soc.* **2013**, *135*, 11525–11528; A. C. Filippou, B. Baars, O. Chernov, Y. N. Lebedev, G. Schnakenburg, *Angew. Chem. Int. Ed.* **2014**, *53*, 565–570; Y. N. Lebedev, U. Das, G. Schnakenburg, A. C. Filippou, *Organometallics* **2017**, *36*, 1530–1540.
- [11] A. Amgoune, D. Bourissou, *Chem. Commun.* **2011**, *47*, 859–871.
- [12] J. Bauer, H. Braunschweig, R. D. Dewhurst, *Chem. Rev.* **2012**, *112*, 4329–4346.
- [13] J. Campos, *J. Am. Chem. Soc.* **2017**, *139*, 2944–2947.
- [14] a) “Organometallic Platinum(II) and Palladium(II) Complexes as Donor Ligands for Lewis-Acidic d10 and s2 Centers; in Higher Oxidation State Organopalladium and Platinum Chemistry”: M. E. Moret, *Topics in Organometallic Chemistry*, Vol. 35. (Ed.: A. Canty), Springer, Berlin, **2011**; b) J. F. Plummer, E. P. Schram, *Inorg. Chem.* **1975**, *14*, 1505–1512; c) J. Bauer, H. Braunschweig, P. Brenner, K. Kraft, K. Radacki, K. Schwab, *Chem. Eur. J.* **2010**, *16*, 11985–11992; d) H. Braunschweig, R. D. Dewhurst, *Dalton Trans.* **2011**, *40*, 549–558; e) B. R. Barnett, J. S. Figueroa, *Chem. Commun.* **2016**, *52*, 13829–13839.
- [15] For examples of tetrahedral Ni⁰ complexes bearing tetrylene ligands, see: a) M. Veith, L. Stahl, V. Huch, *J. Chem. Soc. Chem. Commun.* **1990**, 359–361; b) W. A. Herrmann, M. Denk, J. Behm, W. Scherer, F.-R. Klingan, H. Bock, B. Solouki, M. Wagner, *Angew. Chem. Int. Ed. Engl.* **1992**, *31*, 1485–1488; c) A. G. Avent, B. Gehrhus, P. B. Hitchcock, M. F. Lappert, H. Maciejewski, *J. Organomet. Chem.* **2003**, *686*, 321–331.
- [16] For examples of trigonal planar Ni⁰ systems bearing tetrylene ligands, see: a) P. Bender, A. J. Shusterman, M. M. Banaszak Holl, J. W. Kampf, *Organometallics* **1999**, *18*, 1547–1552; b) C. Watanabe, Y. Inagawa, T. Iwamoto, M. Kira, *Dalton Trans.* **2010**, *39*, 9414–9420; c) T. J. Hadlington, T. Szilvási, M. Driess, *Angew. Chem. Int. Ed.* **2017**, *56*, 7470–7474.
- [17] C. Gendy, A. Mansikkam-ki, J. Valjus, J. Heidebrecht, P. C.-Y. Hui, G. M. Bernard, H. M. Tuononen, R. E. Wasylshen, V. K. Michaelis, R. Roesler, *Angew. Chem. Int. Ed.* **2019**, *58*, 154–158.
- [18] M. Frutos, N. Parvin, A. Baceiredo, D. Madec, N. Saffon-Merceron, V. Branchadell, T. Kato, *Angew. Chem. Int. Ed.* **2022**, *61*, e202201932.

- [19] S. Takahashi, M. Frutos, A. Baceiredo, D. Madec, N. Saffon-Merceron, V. Branchadell, T. Kato, *Angew. Chem. Int. Ed.* **2022**, *61*, e202208202.
- [20] H. Braunschweig, M. A. Celik, R. D. Dewhurst, M. Heid, F. Huppa, S. S. Sen, *Chem. Sci.* **2015**, *6*, 425–435.
- [21] D. Heitmann, T. Pape, A. Hepp, C. Mück-Lichtenfeld, S. Grimme, F. E. Hahn, *J. Am. Chem. Soc.* **2011**, *133*, 11118–11120.
- [22] a) P. M. Keil, T. J. Hadlington, *Angew. Chem. Int. Ed.* **2022**, *61*, e202114143; b) P. M. Keil, T. J. Hadlington, *Chem. Commun.* **2022**, *58*, 3011–3014.
- [23] M. Auer, J. Bolten, K. Eichele, H. Schubert, C. P. Sindlinger, L. Wesemann, *Chem. Sci.* **2023**, *14*, 514–524.
- [24] P. M. Keil, T. J. Hadlington, *Z. Anorg. Allg. Chem.* **2022**, *648*, e202200141.
- [25] M. R. Elsby, S. A. Johnson, *J. Am. Chem. Soc.* **2017**, *139*, 9401–9407.
- [26] We have recently reported a similar utility for the closely related Fe⁰ complex, IPr-Fe(vtms)₂, which can act as in IPr-Fe⁰ transfer reagent: P. M. Keil, A. Soyemi, K. Weisser, T. Szilvási, C. Limberg, T. J. Hadlington, *Angew. Chem. Int. Ed.* **2023**, *62*, e202218141.
- [27] These complexes can also be accessed using the isolated cationic tetrylenes [^{PhIP}DippE][BAR^{F₄}], see ref. [24].
- [28] Deposition Numbers 2239748 (for **3a**), 2239749 (for **3b**), 2239750 (for **3c**), 2239751 (for **4a**), 2239752 (for **4b**), 2239753 (for **5**), 2239754 (for **7**), 2239755 (for **8**), 2239756 (for **9**), 2239757 (for **10**), and 2239758 (for **11**) contains the supplementary crystallographic data for this paper. These data are provided free of charge by the joint Cambridge Crystallographic Data Centre and Fachinformationszentrum Karlsruhe Access Structures service.
- [29] Y. Hoshimoto, Y. Hayashi, H. Suzuki, M. Ohashi, S. Ogoshi, *Organometallics* **2014**, *33*, 1276–1282.
- [30] Binding energies were defined through non-isodesmic methods, at the ωB97XD//def2svp level of theory; see the Supporting Information for more details.
- [31] a) C. Ganesamoorthy, J. Schoening, C. Wölper, L. Song, P. R. Schreiner, S. Schulz, *Nat. Chem.* **2020**, *12*, 608–614; b) D. Reiter, R. Holzner, A. Porzelt, P. Frisch, S. Inoue, *Nat. Chem.* **2020**, *12*, 1131–1135.
- [32] We note that the related reaction for **4a** initially forms a single reaction product, which undergoes rapid decomposition in solution, and thus could not be isolated.
- [33] a) M. R. Elsby, R. T. Baker, *Chem. Soc. Rev.* **2020**, *49*, 8933–8987; b) R. J. Somerville, J. Campos, *Eur. J. Inorg. Chem.* **2021**, 3488–3498; c) Y. Wang, A. Kostenko, S. Yao, M. Driess, *J. Am. Chem. Soc.* **2017**, *139*, 13499–13506.
- [34] This screening was conducted with 5 mol % **5**, for 4 h.
- [35] The cyclic alkene, cyclopentene, was also screened as a substrate in this catalysis, which led to oligomerisation, and only a small degree (≈6%) of hydrogenation. See Figures S116, S127, and S128 in the Supporting Information for more information.
- [36] a) P. J. Chirik, *Acc. Chem. Res.* **2015**, *48*, 1687–1695; b) T. D. Zell, D. Milstein, *Acc. Chem. Res.* **2015**, *48*, 1979–1994; c) S. Weber, B. Stöger, L. F. Veiros, K. Kirchner, *ACS Catal.* **2019**, *9*, 9715–9720.
- [37] J. R. Ludwig, C. S. Schindler, *Chem* **2017**, *2*, 313–316.
- [38] Given that ammonia complexes are unstable at ambient temperature, and DMAP adduct **11** is unstable at elevated temperatures, these bases could not be studied under the catalytic conditions.
- [39] That is, NMR spectroscopic analysis of these mixtures does not show a shift in the characteristic peaks in ¹H and ³¹P{¹H} NMR spectra.

Manuscript received: April 28, 2023
Accepted manuscript online: May 17, 2023
Version of record online: June 28, 2023